ACS ES&T Water

pubs.acs.org/estwater

Article

Fast Multielement Quantification of Nanoparticles in Wastewater and Sludge Using Single-Particle ICP-MS

Yuxiong Huang, Arturo A. Keller,* Pabel Cervantes-Avilés, and Jenny Nelson

Cite This: https://dx.doi.org/10.1021/acsestwater.0c00083

Read Online

ACCESS | Metrics & More | Article Recommendations | Supporting Information

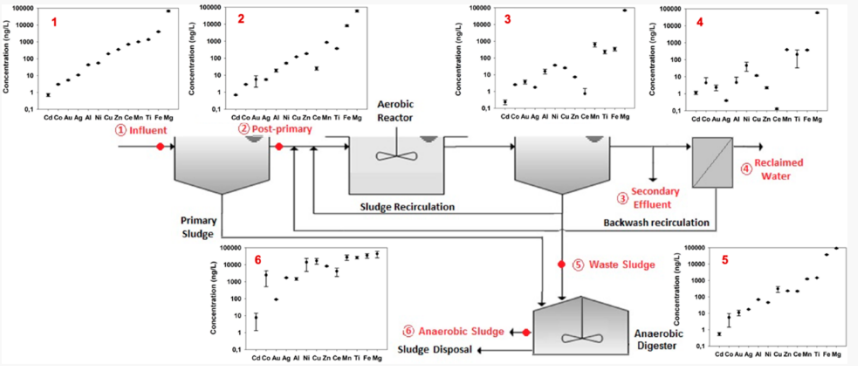

ABSTRACT: Quantitatively monitoring the presence of engineered, natural, or incidental nanoparticles (NPs) is essential to understand their potential environmental and ecotoxicological implications. In particular, a significant number of NPs may travel through wastewater treatment plants (WWTPs), as a conduit to their release to the environment, either in treated effluent or in wastewater sludge (biosolids). Here we developed a fast and simple protocol for full quantitative multielement analysis of metallic or metal-containing NPs in wastewater and sludge samples via single-particle ICP-MS. We employed centrifugation to separate NPs from wastewater sludge, with high recoveries (>84%) for Au and Ag NPs, which have rather high densities (19.3 and 10.5 g cm^{-3}, respectively). In wastewater samples, particle mass concentrations ranged from <1 ng/L for Cd-based NPs to almost 100 μg/L for Mg particles. Particles from most elements detected in wastewater were <100 nm in size, although TiO_2 in raw wastewater was around 250 nm in size, and Mg was >1500 nm in size, well beyond the nanoscale. The efficiency of removal of NPs throughout the WWTP was significantly dependent on the type of metal-containing particles and the influent concentration.

KEYWORDS: *multielement spICP-MS, wastewater, sludge, nanoparticle, separation, retention*

INTRODUCTION

Over the past decade, knowledge about the potential implications of engineered nanomaterials (ENMs) has grown at a fast pace, generating the ability to make predictions about their potential human and ecological risks.[1−7] However, the ability to reliably detect and quantify the presence of nanoparticles (NPs) in the aquatic environment and in anthropogenic flows to the environment has proven to be much more challenging. Thus, evaluating model predictions with reliable measurements is key for improving our understanding of the risks posed by ENMs.

The increasing use of ENMs in common consumer products, such as food and personal care products,[8−11] is a cause for concern. After the use of these products, the embedded ENMs enter the wastewater stream and eventually pass through the sewer systems and wastewater treatment plants (WWTPs).[12−15] Although material flow analyses can generate predicted environmental concentrations (PECs),[13] there is a clear need to measure actual concentrations, to validate models and assumptions.

Within the WWTP, the average hydraulic retention time (HRT) from pretreatment to secondary clarifier is typically 6−24 h,[16] and the sludge retention times (SRT) could be up to 14 days.[17] Because the NPs are subjected to a number of processes,[18−21] including agglomeration, aggregation, coating with organic matter, and transformations (via both dissolution and redox processes), only a small fraction of the initial NPs in consumer products generally remains in the treated effluent, while the majority is transferred to the sludge, in many cases, significantly transformed.[22] Although a number of recent

Received: July 29, 2020
Revised: September 2, 2020
Accepted: September 16, 2020

studies have measured NP concentrations of a few elements in treated effluent,[23,24] only a few studies have applied the spICP-MS for the quantification of NPs in wastewater sludge[25] and biosolids.[26] Because the microorganisms involved in wastewater are artifacts during quantification of NPs, imaging the NPs in the sludge[27,28] or biosolid samples[29] via electron microscopy is a reproducible approach to confirm the presence of NPs in such media but limited for quantification. Therefore, there is also a need to exclude the biomass involved in wastewater treatment to quantify the NPs in wastewater. Some studies have indicated that filtration prior to spICP-MS reveals adsorptive loss of the NPs,[30,31] which influence the concentration measured of NPs. New approaches to separate the biomass from NPs should be conducted.

Because PECs of NPs in the effluent of WWTPs are predicted to be in the range from nanograms per liter to micrograms per liter,[7,10,14] it has been a major challenge for conventional NP characterization methods to detect them and provide accurate, quantitative concentrations. Dynamic light scattering (DLS), transmission electron microscopy (TEM), and differential centrifugal sedimentation (DCS) cannot practically achieve these low concentrations; nanoparticle tracking analysis (NTA) can detect NPs in this range but provides no information about NP composition. Single-particle inductively coupled plasma mass spectrometry (spICP-MS) has gone from being a technique developed in a few research laboratories[31−35] to a viable approach applied in many laboratories for detecting metallic NPs in many matrices.[23,30,36−41] spICP-MS provides the mass and number concentration of NPs, the background dissolved ion concentration, the size of the NPs (assuming a spherical NP, which may not be accurate), and the elemental mass fraction. Detection is best at low concentrations (nanograms per liter to micrograms per liter), making it ideal given the PECs; it actually requires dilution if the samples are expected to be at higher concentrations.

Until recently, spICP-MS could detect only a single element per run. The user would have to select a specific element and isotopic composition for the NP of interest. However, most environmental samples, including wastewater and wastewater sludge, usually contain very diverse NPs, with different elemental and/or isotopic compositions. Although the sample can be run several times to detect NPs with different elements,[35] this entails a much longer analytical time. The ability to detect more than one element, or several isotopes of a given element, can help to identify the source of the NPs. ICP coupled with time-of-flight mass spectrometry (ICP-TOFMS) is an alternative solution to overcome the single-isotope restrictions of conventional ICP-MS instruments for spICP-MS analysis.[42] spICP-TOFMS can be applied to detect different NPs simultaneously, with some trade-offs such as data analysis, a lower sensitivity for some elements, and drift.[43]

Given the fast acquisition time of state-of-the-art ICP-MS, it has recently become feasible to collect signals for up to 16 different elements or isotopes consecutively in the same sample run (sequential acquisition within 100−500 μs).[44] Just as in single-element analysis (i.e., only one element collected in a run), data needed to estimate particle size, particle concentration, and particle distribution for each element can be collected at the same time, with only a need to have the computing power to extract the information from the acquired signals. Compared to acquiring NP data separately for each element of interest,[35] the multielement approach simplifies the analytical protocol and shortens data acquisition and processing times considerably.

In this study, we applied multielement spICP-MS to detect and quantify NPs within real wastewater and wastewater sludge samples. We developed a simple sample pretreatment of sludge to separate the NPs, which we validated with recovery studies of high-density NPs. We then determined the presence of 13 different common types of metal-based NPs in the wastewater treatment process, including the aqueous streams and the sludges.

MATERIALS AND METHODS

Reagents. Ultrapure water (deionized) was obtained from a Barnstead NANOpure water purification system (Thermo Scientific, Boston, MA) and used throughout this work. Nitric acid (67−70% HNO_3) of ultrahigh purity for quantitative trace metal analysis at the parts per trillion level (BDH Aristar Ultra grade) was used to prepare ionic calibration standards. Certified individual ICP-MS ionic calibration standards containing 100 mg/L gold (Au), 10 mg/L silver (Ag) in 2% HNO_3, and a multielement calibration standard containing 10 mg/L aluminum (Al), cadmium (Cd), cerium (Ce), cobalt (Co), copper (Cu), iron (Fe), magnesium (Mg), manganese (Mn), nickel (Ni), titanium (Ti), and zinc (Zn) in a matrix of 5% HNO_3 were purchased from Agilent Technology (Santa Clara, CA).

Nanomaterials. Two gold NPs, with nominal diameters of 60 ± 4 and 30 ± 3 nm, and one silver NP, with a nominal diameter of 60 ± 4 nm, were purchased from nanoComposix (San Diego, CA) as bare, dispersible, gold, and silver nanospheres in aqueous solution (2 mM sodium citrate).

Wastewater and Waste Sludge Samples. Wastewater and waste sludge samples were collected from a WWTP in southern California. Samples were collected from six points within the treatment process (as shown in Figure S1): (1) influent, (2) postprimary, (3) secondary effluent, (4) reclaimed after ultrafiltration, (5) waste sludge from secondary treatment, and (6) anaerobic sludge from the sludge digester. Polyethylene containers (1 L) with polypropylene caps were rinsed and stored in plasma pure grade nitric acid (10%) overnight before the sampling day. On site, the containers were rinsed three times with the respective wastewater or sludge samples before they were filled, and samples were stored at 4 °C until their analysis by multielement spICP-MS and physicochemical characterization.

Separation of NPs from Wastewater Sludge. To separate the NPs from sludge, the samples were centrifuged at different speeds (2500, 5000, and 10000 rpm, equivalent to 949*g*, 3796*g*, and 15180*g*, respectively) and times (5, 10, and 20 min) in a superspeed centrifuge (RC-5B plus, Sorvall) with a fixed angle (23°) rotor (SLA-1500, Thermo Scientific).

Au NPs, used as reference materials, were spiked into wastewater sludge samples before and after the separation process, to obtain pre- and postseparation spike recoveries, and determine the optimal conditions for separation. Two different sizes of Au NPs (30 and 60 nm) were spiked into the wastewater sludge samples to evaluate the optimized separation method for recovering different size ENMs. The concentration of Au NPs spiked into the samples was 100 ng of Au/L. After centrifugation, the supernatant was analyzed via multielement spICP-MS. The recoveries were calculated using eq S1.

https://dx.doi.org/10.1021/acsestwater.0c00083
ACS EST Water XXXX, XXX, XXX−XXX

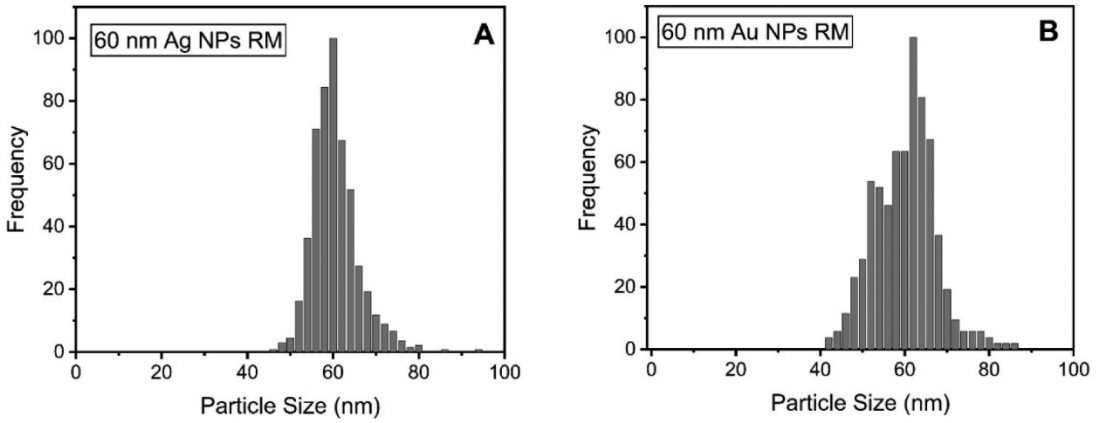

Figure 1. Size distribution of 60 nm reference materials in DI water measured in multielement spICP-MS mode: (A) Ag NPs and (B) Au NPs. Frequency indicates the number of detected NPs in each particle size bin, normalized by the most frequently detected particle size. A minimum of 100 particles were considered, and in some cases, >1000 NPs were measured.

Table 1. NP Centrifugation Conditions and Recoveries for Au Spiked into Sludge (n = 3 for each condition)[a]

		precentrifugation spike			postcentrifugation spike		
centrifugation speed (rpm)	centrifugation time (min)	median size (nm)	mean size (nm)	recovery (%)	median size (nm)	mean size (nm)	recovery (%)
2500	10	54 ± 1	53 ± 1	65 ± 3.2	54 ± 0	54 ± 0	92 ± 3.4
5000	5	54 ± 1	54 ± 0	59 ± 1.3	55 ± 0	54 ± 0	91 ± 4.3
5000	10	55 ± 1	55 ± 0	64 ± 3.0	55 ± 0	55 ± 0	97 ± 0.4
5000	20	55 ± 0	54 ± 0	64 ± 2.3	55 ± 0	55 ± 0	107 ± 2.8
10000	10	54 ± 2	54 ± 2	11 ± 0.26	55 ± 0	54 ± 0	86 ± 2.6

[a]Standard deviations of the values are given.

NP sample preparation and dilution were performed on the day of the analysis to avoid sample degradation and minimize the potential dissolution of NPs after processing. Before dilution of the samples and again prior to their analysis, all solutions were placed in an ultrasonic bath for 10 min, to ensure that the samples were fully homogenized.

To further evaluate the effectiveness of the separation of NPs from the waste-activated sludge (waste sludge), Au and Ag NPs were spiked into the waste sludge simultaneously, at concentrations of 100 ng of Au/L and 100 ng of Ag/L.

spICP-MS Measurement. An Agilent 7900 ICP-MS instrument equipped with standard nickel sampling and skimmer cones, a standard glass concentric nebulizer, a quartz spray chamber, and a quartz torch [with a small internal diameter (1.0 mm) injector] was used to perform multielement spICP-MS analysis to determine the NP composition, size, and concentration in all samples. Samples were introduced directly into the ICP-MS instrument with the standard peristaltic pump and tubing (internal diameter of 1.02 mm). Analyses were performed using the Rapid Multi-Element Nanoparticle Analysis mode of the Single Nanoparticle Application Module of the Agilent ICP-MS MassHunter software (version C.01.05, build 588.3). Data on the elements of interest were collected sequentially in time-resolved analysis (TRA) mode using an integration time (dwell time) of 100 μs per point with no settling time between readings, and 15 s of lag time between masses. The instrumental settings used for the spICP-MS analysis are summarized in Table S5.

pICP-MS detects and analyzes individual nanoparticles, allowing for the determination of the number of nanoparticles, the distribution and size of the nanoparticles, and the concentration of the element(s) present in each nanoparticle. In this technique, a flow of diluted, suspended, nanoparticles is introduced into the ICP-MS plasma, via the sample introduction setup. If the nanoparticle sample suspension is appropriately diluted, only one particle is introduced into the plasma at each time point. As individual nanoparticles enter the plasma, they produce a flash of ions that generate a large transient signal. Acquisition of each of these events in time-resolved acquisition (TRA) mode allows the determination of the number of particles in a given sample volume.

The signal intensity of each measured NP is then converted to a mass, using information from the reference material (Au NP, 60 nm), the nebulization efficiency (calculated using eq S2), and the determination of the baseline for each element. The mass concentration of the NPs can be calculated by integrating the peaks identified for a given NP.

In this study, the reference material was 60 nm Au NP reference material (nanoComposix) in deionized (DI) water. The reference material was diluted to 100 ng of Au/L with DI water in metal-free polypropylene tubes. The nebulization efficiency was determined to be 0.065 for the Agilent 7900 instrument with the operating conditions indicated in Table S5. A sample inlet flow of 0.346 mL/min was used. To determine the elemental response factor (R) for each analyte, a multielement ionic standard containing all analytes of interest (10 mg/L) was first diluted to 1 μg/L with 1% HNO_3. The response factors are listed in Table S3. The average ionic background for each of the elements of interest in the sample was determined by measuring the signal between nanoparticle peaks. The dissolved ionic concentration is determined using eq S3.

To calculate the particle size from the particle mass using the spICP-MS software, we had to make some assumptions, as

https://dx.doi.org/10.1021/acsestwater.0c00083
ACS EST Water XXXX, XXX, XXX−XXX

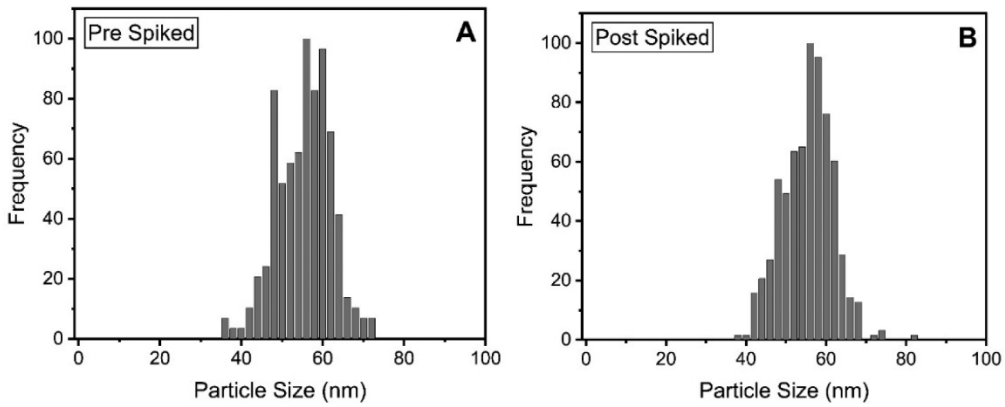

Figure 2. Size distribution of 60 nm Au NP reference materials spiked at 100 ng/L detected in the retentate of activated waste sludge after centrifugation: (A) precentrifugation and (B) postcentrifugation. Centrifugation was performed at 5000 rpm for 10 min.

previously considered by others,[45,46] regarding (1) the chemical composition and density of each metal-based nanoparticle (Table S4) and (2) the spherical shape of the NPs. Given the measured mass of a NP, its density based on the assumed composition, and the assumed spherical shape, the volume of the sphere can be determined, and a nominal diameter can be estimated. In addition, we assumed only one element of interest was present in each type of NPs; this is a simplification because most commercial NPs will have impurities, but without more information about the source of the NPs in the WWTP stream, at present one cannot assume a mixed elemental composition.

Each sample was analyzed in triplicate via spICP-MS to obtain the mean and standard deviation of the particle number and mass concentration. The samples were diluted with DI water to ensure the NP concentrations were between 10 and 100 ng/L.

RESULTS

Multielement spICP-MS Measurement Accuracy. After spiking 60 nm Ag and 60 nm Au reference NPs into DI water, we analyzed the samples with the multielement spICP-MS method. The size distributions of Ag and Au reference materials were obtained in one sample acquisition (Figure 1). For the Ag NPs, the measured mean size of 59 ± 1 nm and the median size of 58 ± 1 nm (±standard deviation of mean and median size, respectively) agreed with the certificate values obtained via TEM (59 ± 5 nm) and DLS (hydrodynamic diameter of 60 nm) provided by the manufacturer. A similar accuracy was achieved for the 60 nm Au NP reference materials, with measured mean and median sizes of 61 ± 1 and 58 ± 0 nm, respectively, while the certificate values from the manufacturer were 60 ± 6 nm (TEM).

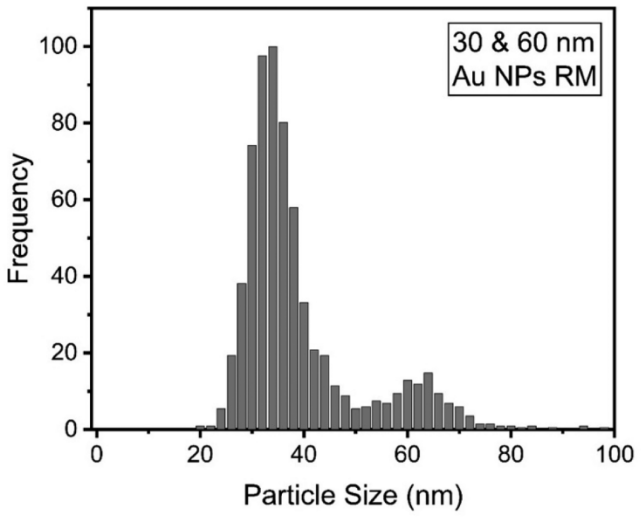

Figure 3. Size distribution of Au NPs with two different sizes (30 and 60 nm) spiked precentrifugation into waste sludge samples. Centrifugation was performed at 5000 rpm for 10 min.

Recovery of NPs from Complex Environmental Matrices. WWTP sludge is a rather complex matrix, with a very high content of solids, as well as chemical oxygen demand and organic carbon content. Tables S1 and S2 present the characterization of the wastewaters and sludges used in this study. Centrifugation can provide a fast and simple approach for separating free NPs within waste sludge samples. To evaluate and validate the NP separation method, three replicates of each sludge sample were spiked with 100 ng/L 60 nm Au NP reference material and then centrifuged using different centrifugation speeds and times (Table 1).

The recovery of the precentrifugation Au NP spike varied significantly as the centrifugation speed was increased from 2500 to 10000 rpm, at a constant centrifugation time (10 min). Notably, only 11% of the precentrifugation spiked Au NPs were recovered at 10000 rpm (Table 1). No statistically significant difference in recovery was observed by increasing the speed from 2500 to 5000 rpm, with ∼65% of the precentrifugation Au NPs remaining in the supernatant after centrifugation. Adjusting the centrifugation time from 5 to 20 min at 5000 rpm indicated that while 10 min was better than 5 min, there was no benefit in increasing the time to 20 min. Au NPs spiked postcentrifugation were recovered substantially, from 85% to 107% under all tested conditions, indicating a negligible matrix effect in sludge retentate. Median and mean sizes of spiked Au NPs pre- and postcentrifugation were also determined by spICP-MS under all test conditions (Table 1). As demonstrated, the ENM extraction protocol, using centrifugation to physically extract ENMs from sludge prior to introducing the sample into the LC-MS instrument, does not influence the size measurements. The protocol does not affect the spICP-MS nebulization transport efficiency and can be applied in the extraction of other ENMs.

https://dx.doi.org/10.1021/acsestwater.0c00083
ACS EST Water XXXX, XXX, XXX−XXX

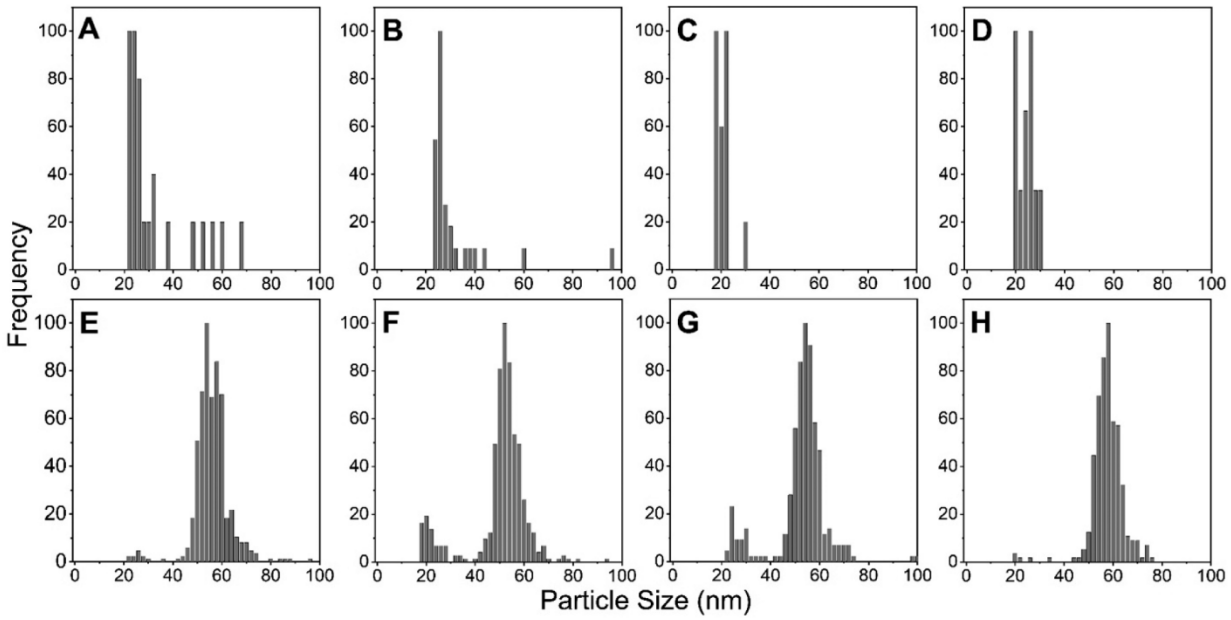

Figure 4. Ag NP size distribution in unspiked (A) influent, (B) postprimary, (C) waste sludge, and (D) anaerobic sludge and in spiked (E) influent, (F) postprimary, (G) waste sludge, and (H) anaerobic sludge.

Table 2. Concentrations of Ag NPs in Wastewater and Sludge Samples, as Sampled and Spiked Pre- and Postcentrifugation

	concentration in unspiked samples (ng/L)	precentrifugation spike recovery (%)	postcentrifugation spike recovery (%)
influent	12 ± 0.6	66 ± 2.1	99 ± 1.3
postprimary	1.1 ± 0.2	84 ± 1.1	100 ± 2.3
waste sludge	4.5 ± 0.5	41 ± 3.8	72 ± 2.7
anaerobic sludge	494 ± 6.4	64 ± 2.5	93 ± 1.0

The time-resolved data for Au NPs in sludge samples exhibit few peaks for the unspiked sludge sample (Figure S2A), because Au-containing/Au NPs were rarely detected in the sludge of the WWTP. The majority of the signal was background noise, and the baseline was determined by the sequential removal of the signal above baseline until a stable baseline was achieved. The threshold is set where the actual signal distribution curve starts to separate from the estimated background curve at the slope of points near zero. As shown in Table S6, only ∼1 particle per liter was detected in the as-collected samples, while 206 and 408 particles per liter were detected in the pre- and postcentrifugation sludge samples, respectively, which agrees with the peaks observed in Figure S2A−C.

The measured dissolved ionic concentrations were comparable to the particle mass concentration (Table S6), indicating acceptable signal separation relative to noise. The background equivalent diameter (BED), d_{bkgnd} (calculated via eq S4), is another important criterion for determining the cutoff between the signals of the particles and dissolved ions and permits an estimation of the approximate minimum particle size detection limit. Because the reported BEDs (Table S6) are much smaller than the nominal and measured Au NP size (Table 1), this indicates high precision in the size determination for the Au NPs using spICP-MS even in the sludge matrix.

The sizes of spiked Au NPs measured in the sludge supernatant were very close to those measured in DI water (Figure 1B), although with a trend toward smaller median and mean sizes, indicating that the Au NPs transferred to the sludge solids were, on average, the larger particles. Considering the balance of maximizing the retention of NPs in the supernatant and minimizing retention in the solid phase, centrifuging the sludge samples at 5000 rpm for 10 min was chosen as the optimal pretreatment protocol. Using the proposed pretreatment, the size distribution of pre- and postcentrifugation spiked Au NP reference materials did not exhibit substantial differences (Figure 2).

Recovery of Multielement NPs from Complex Matrices. To determine if NPs of different sizes could be robustly differentiated after separation from a complex matrix, such as sludge, using the separation protocol (centrifugation at 5000 rpm for 10 min), we evaluated the recovery efficiency of 30 and 60 nm Au NP reference materials, which were spiked into waste sludge samples. Two clear peaks at 36 and 64 nm were observed (Figure 3), indicating that spICP-MS can provide high-resolution size determination for NPs in wastewater and sludge samples, even at low (environmentally relevant) concentrations.

In addition to the 30 and 60 nm Au NPs, 60 nm Ag NPs were spiked precentrifugation at 100 ng/L Ag into the wastewater (influent and postprimary) and sludge (waste and anaerobic) samples to evaluate the capability of the protocol to recover NPs of different elemental compositions from the complex environmental matrix. There is a clear difference in the Ag NP size distribution between the unspiked samples (Figure 4A−D) and the spiked ones (Figure 4E−H), with a clear second peak for the spiked Ag NPs centered slightly below 60 nm.

The mass concentration of Ag NPs ranged from 1.1 to 493 ng/L, with the highest concentration in anaerobic sludge (Table 2), which reflects the transfer of Ag NPs from the influent aqueous stream to the biosolids. The recovery of precentrifugation spiked Ag NPs was higher in the aqueous

https://dx.doi.org/10.1021/acsestwater.0c00083
ACS EST Water XXXX, XXX, XXX−XXX

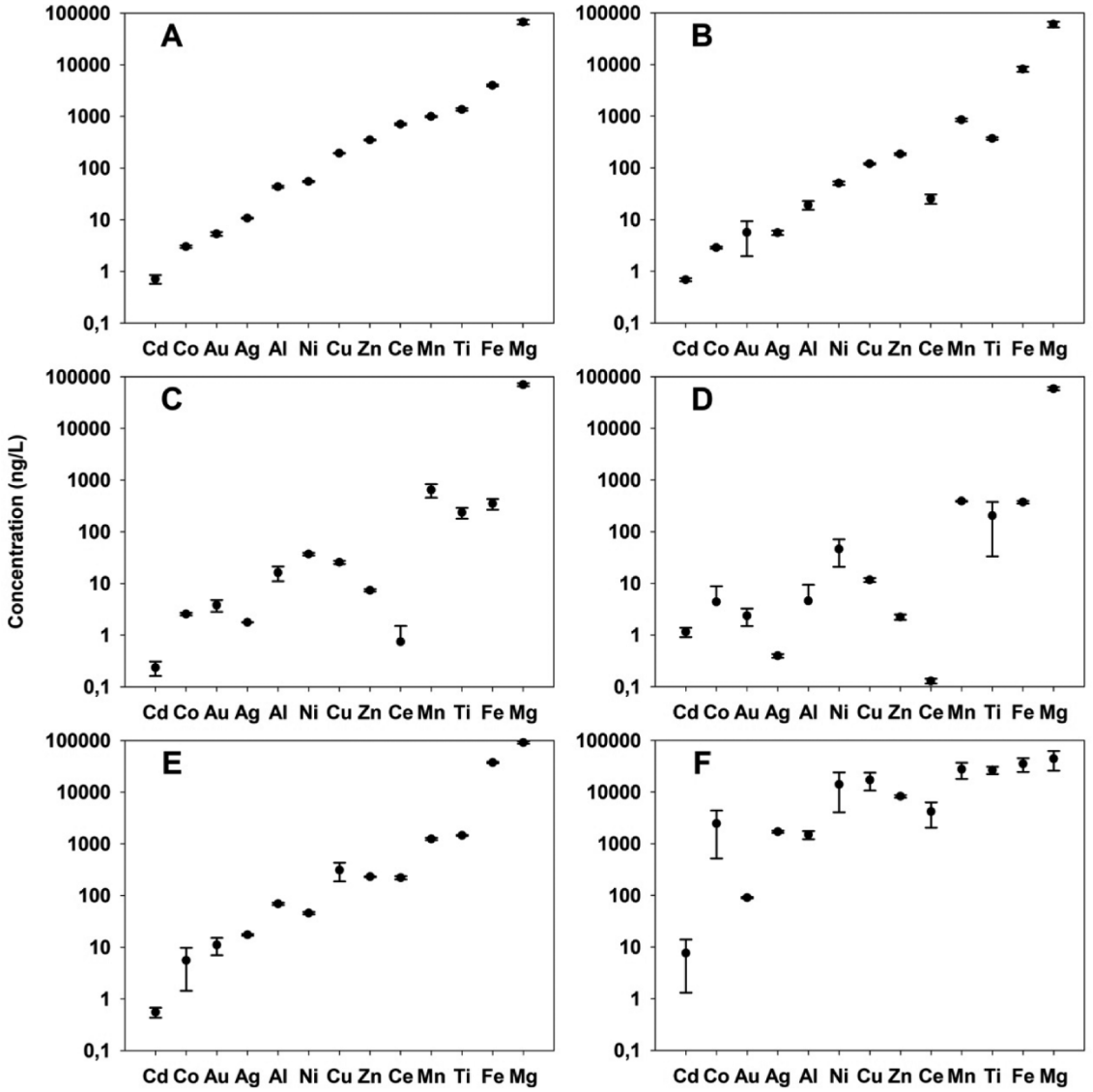

Figure 5. Mass concentration of NPs at different stages of wastewater treatment: (A) influent, (B) postprimary, (C) seconday effluent, (D) reclaimed water, (E) spiked waste sludge, and (F) spiked anaerobic sludge. Error bars indicate one standard deviation.

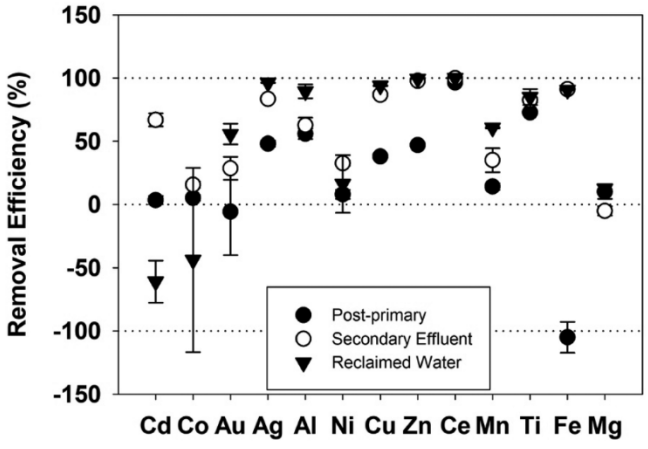

Figure 6. Removal efficiency of different NPs based on influent concentrations.

streams (influent and postprimary); there was more retention in the waste sludge solids.

Detection of NPs in Wastewater and Sludge. The multielement spICP-MS analysis of the wastewater and supernatant of centrifuged sludge samples resulted in a wide range of concentrations of different particles, with cadmium at the lower end, <1.0 ng/L in the influent, and magnesium at the high end, almost 100 μg/L (Figure 5A). TEM confirmed the presence of electron-dense material nanoparticulate in the influent (Figure S3A−D). Table S7 presents the mean and standard deviation of measured NP mass concentration values, while the ionic concentration is listed in Table S9. As expected, there was a decrease in concentration (Figure 6) in the aqueous stream as it proceeds through the treatment processes (influent > postprimary > secondary effluent > reclaimed), with an accumulation of NPs in the waste and anaerobic sludges, although the removal efficiency was strongly dependent on elemental composition (Figure 7). Note that the "negative" removal of Cd and Co NPs reflects the uncertainty of the measured concentrations, because these NPs were around 1−3 ng/L in the influent. Mg removal is negligible, given its very high influent concentration.

https://dx.doi.org/10.1021/acsestwater.0c00083
ACS EST Water XXXX, XXX, XXX−XXX

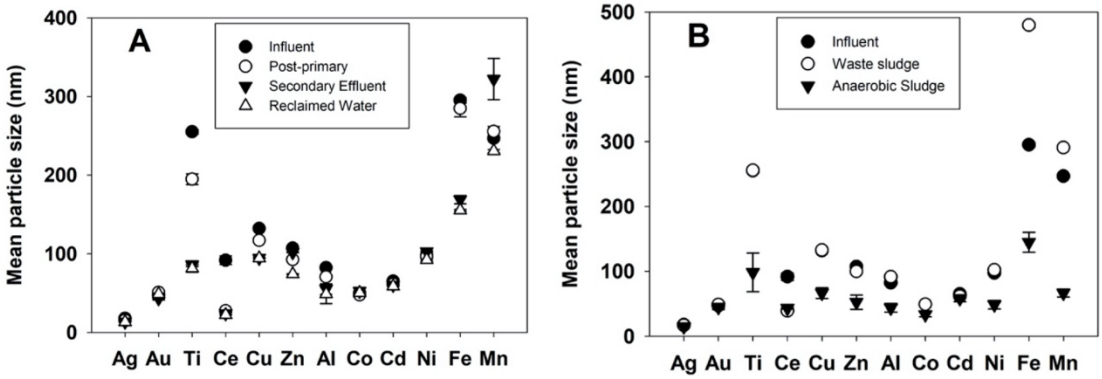

Figure 7. Particle size (mean and standard deviation) at different stages of treatment: (A) aqueous streams and (B) sludges, with influent for reference. Error bars indicate one standard deviation.

Particle sizes for nine elements (Ag, Al, Au, Cd, Ce, Co, Cu, Ni, and Zn) were generally <100 nm, particularly in the aqueous stream as treatment progressed (Figure 7A). Ti particles, likely TiO_2, were detected at 255 ± 3 nm in the influent, which is expected for agglomerated NPs, but by the effluent the particle size was around 86 ± 2 nm. Fe and Mn particles were within 200 and 400 nm, decreasing to the lower end of the range after ultrafiltration for reclaimed water. In the waste sludge, the mean particle size remained the same or increased, relative to that of the influent, but generally decreased in the anaerobic sludge relative to the influent (Figure 7B). Mg particles are not presented in Figure 7, because they were consistently above 1500 nm throughout the entire process. The data are listed in Table S8, and the BED data are listed in Table S10.

DISCUSSION

While we demonstrate that multielement spICP-MS is capable of detecting a large number of NPs of different elemental compositions, further work will be needed to discern whether these are manufactured, natural, or incidental NPs. For many metal-based NPs (e.g., Fe, Al, and Mg), the background concentration of natural NPs will likely dominate in these real samples. In addition, a number of NPs are manufactured with core−shell configurations, with different elements in the core and shell, which will complicate the analysis, although it may shed light on whether they are natural or manufactured.

The background ionic concentration can also present a challenge for some elements, limiting the ability to detect smaller NPs. The minimum detectable size for each element depends on the level of ionic concentration and other background noise. We also noticed that particular metal-based NPs (e.g., Fe and Mn), which were present in wastewater and sludge samples at higher concentrations (from parts per trillion to sub-parts per million), usually exhibited larger particle sizes. It may be attributed to a higher degree of aggregation during the transport of these NPs in the wastewater treatment plant due to their higher concentrations.

There are a number of important assumptions, in particular the elemental speciation and the spherical shape. These assumptions influence the determination of the particle size, although they do not affect the particle number or mass concentrations. For a sample taken from a WWTP or natural waters that receive WWTP effluent, it will be challenging to verify the validity of these assumptions.

CONCLUSIONS

Multielement spICP-MS can effectively discern NPs of different elemental compositions in a single run, with high accuracy with regard to size distribution, although there is a cutoff at the lower range of the size distribution, which is specific to each element and depends in part on the background ionic concentration of the element. Preprocessing via centrifugation results in a high recovery of the reference NPs.

It should be noted that these results represent the detection of natural, incidental, and engineered NPs. Further work will be needed to discern each NP source, using isotopic ratios as well as mixed elemental composition.[47] The concentrations of the NPs ranged from slightly less than 1 ng/L for Cd-based NPs to nearly 100 μg/L for Mg particles, although these were not NPs, because their average size was >1500 nm. Most of the particles were <100 nm in size, although these estimates are assuming a spherical particle and a particular NP composition and density. Although the removal efficiency of the wastewater treatment process varied significantly on the basis of elemental composition, overall there was a high level of transfer of NPs from the aqueous stream to the sludges. This means that overall the risk of exposure to these metal-based NPs is significantly reduced by the treatment process. Multielement spICP-MS is likely to emerge as the preferred analytical technique for quantifying the presence of NPs in complex matrices, such as wastewater and sludges, providing valuable guidance for the nanoenvironmental health and safety.

ASSOCIATED CONTENT

Supporting Information

The Supporting Information is available free of charge at https://pubs.acs.org/doi/10.1021/acsestwater.0c00083.

A diagram of the treatment process, one figure depicting time-resolved acquisition, and six tables (wastewater and sludge characteristics, assumed properties of the NPs, NP concentrations, and NP size in the treatment steps) (PDF)

AUTHOR INFORMATION

Corresponding Author

Arturo A. Keller − *Bren School of Environmental Science and Management, University of California at Santa Barbara, Santa Barbara, California 93106, United States; Center for Environmental Implications of Nanotechnology, University of*

https://dx.doi.org/10.1021/acsestwater.0c00083
ACS EST Water XXXX, XXX, XXX−XXX

California at Santa Barbara, Santa Barbara, California 93106, United States; orcid.org/0000-0002-7638-662X; Phone: +1 805 893 7548; Email: keller@bren.ucsb.edu; Fax: +1 805 893 7612

Authors

Yuxiong Huang − *Shenzhen Environmental Science and New Energy Technology Engineering Laboratory, Tsinghua-Berkeley Shenzhen Institute, Tsinghua Shenzhen International Graduate School, Shenzhen 518055, P. R. China; Bren School of Environmental Science and Management, University of California at Santa Barbara, Santa Barbara, California 93106, United States; Center for Environmental Implications of Nanotechnology, University of California at Santa Barbara, Santa Barbara, California 93106, United States;* orcid.org/0000-0001-8124-643X

Pabel Cervantes-Avilés − *Bren School of Environmental Science and Management, University of California at Santa Barbara, Santa Barbara, California 93106, United States; Center for Environmental Implications of Nanotechnology, University of California at Santa Barbara, Santa Barbara, California 93106, United States; Tecnologico de Monterrey, Escuela de Ingeniería y Ciencias, CP 72453 Puebla, Pue, Mexico;* orcid.org/0000-0001-9665-2959

Jenny Nelson − *Agilent Technologies Inc., Wilmington, Delaware 19808, United States*

Complete contact information is available at: https://pubs.acs.org/10.1021/acsestwater.0c00083

Notes

The authors declare no competing financial interest.

■ ACKNOWLEDGMENTS

This work was supported by the National Science Foundation (NSF) and the U.S. Environmental Protection Agency (EPA) under Grant NSF-EF0830117. Any opinion, findings, recommendations, or conclusions expressed in this material are those of the authors and do not necessarily reflect the views of the funding agencies. A.A.K. also appreciates Agilent Technologies for their Agilent Thought Leader Award.

■ REFERENCES

(1) Arvidsson, R. Risk Assessments Show Engineered Nanomaterials To Be of Low Environmental Concern. *Environ. Sci. Technol.* **2018**, *52* (5), 2436−2437.

(2) Batley, G. E.; Kirby, J. K.; McLaughlin, M. J. Fate and Risks of Nanomaterials in Aquatic and Terrestrial Environments. *Acc. Chem. Res.* **2013**, *46* (3), 854−862.

(3) Bornhöft, N. A.; Sun, T. Y.; Hilty, L. M.; Nowack, B. A Dynamic Probabilistic Material Flow Modeling Method. *Environ. Model. Softw.* **2016**, *76*, 69−80.

(4) Coll, C.; Notter, D.; Gottschalk, F.; Sun, T.; Som, C.; Nowack, B. Probabilistic Environmental Risk Assessment of Five Nanomaterials (Nano-TiO2, Nano-Ag, Nano-ZnO, CNT, and Fullerenes). *Nanotoxicology* **2016**, *10* (4), 436−444.

(5) Garner, K. L.; Suh, S.; Keller, A. A. Assessing the Risk of Engineered Nanomaterials in the Environment: Development and Application of the NanoFate Model. *Environ. Sci. Technol.* **2017**, *51* (10), 5541−5551.

(6) Keller, A. A.; Parker, N. Chapter 7 - Innovation in Procedures for Human and Ecological Health Risk Assessment of Engineered Nanomaterials. In *Exposure to Engineered Nanomaterials in the Environment*; Marmiroli, N., White, J. C., Song, J., Eds.; Micro and Nano Technologies; Elsevier, 2019; pp 185−208.

(7) Sun, T. Y.; Gottschalk, F.; Hungerbühler, K.; Nowack, B. Comprehensive Probabilistic Modelling of Environmental Emissions of Engineered Nanomaterials. *Environ. Pollut.* **2014**, *185*, 69−76.

(8) Keller, A. A.; Vosti, W.; Wang, H.; Lazareva, A. Release of Engineered Nanomaterials from Personal Care Products throughout Their Life Cycle. *J. Nanopart. Res.* **2014**, *16* (7), 2489.

(9) Song, R.; Qin, Y.; Suh, S.; Keller, A. A. Dynamic Model for the Stocks and Release Flows of Engineered Nanomaterials. *Environ. Sci. Technol.* **2017**, *51* (21), 12424−12433.

(10) Sun, T. Y.; Mitrano, D. M.; Bornhöft, N. A.; Scheringer, M.; Hungerbühler, K.; Nowack, B. Envisioning Nano Release Dynamics in a Changing World: Using Dynamic Probabilistic Modeling to Assess Future Environmental Emissions of Engineered Nanomaterials. *Environ. Sci. Technol.* **2017**, *51* (5), 2854−2863.

(11) Weir, A.; Westerhoff, P.; Fabricius, L.; Hristovski, K.; von Goetz, N. Titanium Dioxide Nanoparticles in Food and Personal Care Products. *Environ. Sci. Technol.* **2012**, *46* (4), 2242−2250.

(12) Gottschalk, F.; Sonderer, T.; Scholz, R. W.; Nowack, B. Modeled Environmental Concentrations of Engineered Nanomaterials (TiO2, ZnO, Ag, CNT, Fullerenes) for Different Regions. *Environ. Sci. Technol.* **2009**, *43* (24), 9216−9222.

(13) Keller, A. A.; Lazareva, A. Predicted Releases of Engineered Nanomaterials: From Global to Regional to Local. *Environ. Sci. Technol. Lett.* **2014**, *1* (1), 65−70.

(14) Lazareva, A.; Keller, A. A. Estimating Potential Life Cycle Releases of Engineered Nanomaterials from Wastewater Treatment Plants. *ACS Sustainable Chem. Eng.* **2014**, *2* (7), 1656−1665.

(15) Mueller, N. C.; Nowack, B. Exposure Modeling of Engineered Nanoparticles in the Environment. *Environ. Sci. Technol.* **2008**, *42* (12), 4447−4453.

(16) Otero-González, L.; Field, J. A.; Sierra-Alvarez, R. Inhibition of Anaerobic Wastewater Treatment after Long-Term Exposure to Low Levels of CuO Nanoparticles. *Water Res.* **2014**, *58*, 160−168.

(17) Kaegi, R.; Voegelin, A.; Sinnet, B.; Zuleeg, S.; Hagendorfer, H.; Burkhardt, M.; Siegrist, H. Behavior of Metallic Silver Nanoparticles in a Pilot Wastewater Treatment Plant. *Environ. Sci. Technol.* **2011**, *45* (9), 3902−3908.

(18) Garner, K. L.; Keller, A. A. Emerging Patterns for Engineered Nanomaterials in the Environment: A Review of Fate and Toxicity Studies. *J. Nanopart. Res.* **2014**, *16* (8), 2503.

(19) Lowry, G. V.; Casman, E. A. Nanomaterial Transport, Transformation, and Fate in the Environment. In *Nanomaterials: Risks and Benefits*; Linkov, I., Steevens, J., Eds.; NATO Science for Peace and Security Series C: Environmental Security; Springer: Dordrecht, The Netherlands, 2009; pp 125−137. DOI: 10.1007/978-1-4020-9491-0_9

(20) Ma, R.; Levard, C.; Judy, J. D.; Unrine, J. M.; Durenkamp, M.; Martin, B.; Jefferson, B.; Lowry, G. V. Fate of Zinc Oxide and Silver Nanoparticles in a Pilot Wastewater Treatment Plant and in Processed Biosolids. *Environ. Sci. Technol.* **2014**, *48* (1), 104−112.

(21) Westerhoff, P.; Song, G.; Hristovski, K. A.; Kiser, M. Occurrence and Removal of Titanium at Full Scale Wastewater Treatment Plants: Implications for TiO 2 Nanomaterials. *J. Environ. Monit.* **2011**, *13* (5), 1195−1203.

(22) Brar, S. K.; Verma, M.; Tyagi, R. D.; Surampalli, R. Y. Engineered Nanoparticles in Wastewater and Wastewater Sludge − Evidence and Impacts. *Waste Manage.* **2010**, *30* (3), 504−520.

(23) Hadioui, M.; Merdzan, V.; Wilkinson, K. J. Detection and Characterization of ZnO Nanoparticles in Surface and Waste Waters Using Single Particle ICPMS. *Environ. Sci. Technol.* **2015**, *49* (10), 6141−6148.

(24) Proulx, K.; Hadioui, M.; Wilkinson, K. J. Separation, Detection and Characterization of Nanomaterials in Municipal Wastewaters Using Hydrodynamic Chromatography Coupled to ICPMS and Single Particle ICPMS. *Anal. Bioanal. Chem.* **2016**, *408* (19), 5147−5155.

(25) Tuoriniemi, J. D.; Jürgens, M.; Hassellöv, M.; Cornelis, G. Size Dependence of Silver Nanoparticle Removal in a Wastewater

Treatment Plant Mesocosm Measured by FAST Single Particle ICP-MS. *Environ. Sci.: Nano* **2017**, *4* (5), 1189−1197.
(26) Jesmer, A. H.; Velicogna, J. R.; Schwertfeger, D. M.; Scroggins, R. P.; Princz, J. I. The Toxicity of Silver to Soil Organisms Exposed to Silver Nanoparticles and Silver Nitrate in Biosolids-Amended Field Soil. *Environ. Toxicol. Chem.* **2017**, *36* (10), 2756−2765.
(27) Cervantes-Avilés, P.; Diaz Barriga-Castro, E.; Palma-Tirado, L.; Cuevas-Rodríguez, G. Interactions and Effects of Metal Oxide Nanoparticles on Microorganisms Involved in Biological Wastewater Treatment. *Microsc. Res. Tech.* **2017**, *80* (10), 1103−1112.
(28) Kim, B.; Park, C.-S.; Murayama, M.; Hochella, M. F. Discovery and Characterization of Silver Sulfide Nanoparticles in Final Sewage Sludge Products. *Environ. Sci. Technol.* **2010**, *44* (19), 7509−7514.
(29) Westerhoff, P.; Lee, S.; Yang, Y.; Gordon, G. W.; Hristovski, K.; Halden, R. U.; Herckes, P. Characterization, Recovery Opportunities, and Valuation of Metals in Municipal Sludges from U.S. Wastewater Treatment Plants Nationwide. *Environ. Sci. Technol.* **2015**, *49* (16), 9479−9488.
(30) Azimzada, A.; Tufenkji, N.; Wilkinson, K. J. Transformations of Silver Nanoparticles in Wastewater Effluents: Links to Ag Bioavailability. *Environ. Sci.: Nano* **2017**, *4* (6), 1339−1349.
(31) Mitrano, D. M.; Lesher, E. K.; Bednar, A.; Monserud, J.; Higgins, C. P.; Ranville, J. F. Detecting Nanoparticulate Silver Using Single-Particle Inductively Coupled Plasma−Mass Spectrometry. *Environ. Toxicol. Chem.* **2012**, *31* (1), 115−121.
(32) Hadioui, M.; Leclerc, S.; Wilkinson, K. J. Multimethod Quantification of Ag+ Release from Nanosilver. *Talanta* **2013**, *105*, 15−19.
(33) Hassellöv, M.; Readman, J. W.; Ranville, J. F.; Tiede, K. Nanoparticle Analysis and Characterization Methodologies in Environmental Risk Assessment of Engineered Nanoparticles. *Ecotoxicology* **2008**, *17* (5), 344−361.
(34) Laborda, F.; Bolea, E.; Jiménez-Lamana, J. Single Particle Inductively Coupled Plasma Mass Spectrometry for the Analysis of Inorganic Engineered Nanoparticles in Environmental Samples. *Trends Environ. Anal. Chem.* **2016**, *9*, 15−23.
(35) Lee, S.; Bi, X.; Reed, R. B.; Ranville, J. F.; Herckes, P.; Westerhoff, P. Nanoparticle Size Detection Limits by Single Particle ICP-MS for 40 Elements. *Environ. Sci. Technol.* **2014**, *48* (17), 10291−10300.
(36) Cervantes-Avilés, P.; Huang, Y.; Keller, A. A. Incidence and Persistence of Silver Nanoparticles throughout the Wastewater Treatment Process. *Water Res.* **2019**, *156*, 188−198.
(37) Hellou, J.; Leonard, J.; Cook, A.; Doe, K.; Dunphy, K.; Jackman, P.; Tremblay, L.; Flemming, J. M. Comparison of the Partitioning of Pesticides Relative to the Survival and Behaviour of Exposed Amphipods. *Ecotoxicology* **2009**, *18* (1), 27.
(38) Keller, A. A.; Huang, Y.; Nelson, J. Detection of Nanoparticles in Edible Plant Tissues Exposed to Nano-Copper Using Single-Particle ICP-MS. *J. Nanopart. Res.* **2018**, *20* (4), 101.
(39) Mitrano, D. M.; Mehrabi, K.; Rojas Dasilva, Y. A.; Nowack, B. Mobility of Metallic (Nano)Particles in Leachates from Landfills Containing Waste Incineration Residues. *Environ. Sci.: Nano* **2017**, *4* (2), 480−492.
(40) Mitrano, D. M.; Ranville, J.; Bednar, A.; Kazor, K. S.; Hering, A. P.; Higgins, C. Tracking Dissolution of Silver Nanoparticles at Environmentally Relevant Concentrations in Laboratory, Natural, and Processed Waters Using Single Particle ICP-MS (SpICP-MS). *Environ. Sci.: Nano* **2014**, *1* (3), 248−259.
(41) Montaño, M. D.; Olesik, J. W.; Barber, A. G.; Challis, K.; Ranville, J. F. Single Particle ICP-MS: Advances toward Routine Analysis of Nanomaterials. *Anal. Bioanal. Chem.* **2016**, *408* (19), 5053−5074.
(42) Borovinskaya, O.; Hattendorf, B.; Tanner, M.; Gschwind, S.; Günther, D. A Prototype of a New Inductively Coupled Plasma Time-of-Flight Mass Spectrometer Providing Temporally Resolved, Multi-Element Detection of Short Signals Generated by Single Particles and Droplets. *J. Anal. At. Spectrom.* **2013**, *28* (2), 226−233.
(43) Praetorius, A.; Gundlach-Graham, A.; Goldberg, E.; Fabienke, W.; Navratilova, J.; Gondikas, A.; Kaegi, R.; Günther, D.; Hofmann, T.; von der Kammer, F. Single-Particle Multi-Element Fingerprinting (SpMEF) Using Inductively-Coupled Plasma Time-of-Flight Mass Spectrometry (ICP-TOFMS) to Identify Engineered Nanoparticles against the Elevated Natural Background in Soils. *Environ. Sci.: Nano* **2017**, *4* (2), 307−314.
(44) Yamanaka, M.; Itagaki, T. Measuring Multiple Elements in Nanoparticles Using SpICP-MS Acquire NP Data for up to 16 Elements in Rapid Multi-Element Nanoparticle Analysis Mode. 2018. https://www.agilent.com/cs/library/applications/application-np-multielement-7900-icp-ms-5994-0310en-us-agilent.pdf.
(45) Laborda, F.; Jiménez-Lamana, J.; Bolea, E.; Castillo, J. R. Critical Considerations for the Determination of Nanoparticle Number Concentrations, Size and Number Size Distributions by Single Particle ICP-MS. *J. Anal. At. Spectrom.* **2013**, *28* (8), 1220.
(46) Pace, H. E.; Rogers, N. J.; Jarolimek, C.; Coleman, V. A.; Higgins, C. P.; Ranville, J. F. Determining Transport Efficiency for the Purpose of Counting and Sizing Nanoparticles via Single Particle Inductively Coupled Plasma Mass Spectrometry. *Anal. Chem.* **2011**, *83* (24), 9361−9369.
(47) Gondikas, A.; von der Kammer, F.; von der Kaegi, R.; Borovinskaya, O.; Neubauer, E.; Navratilova, J.; Praetorius, A.; Cornelis, G.; Hofmann, T. Where Is the Nano? Analytical Approaches for the Detection and Quantification of TiO 2 Engineered Nanoparticles in Surface Waters. *Environ. Sci.: Nano* **2018**, *5* (2), 313−326.

https://dx.doi.org/10.1021/acsestwater.0c00083
ACS EST Water XXXX, XXX, XXX−XXX